Applied Catalysis B: Environmental 119–120 (2012) 156–165

Contents lists available at SciVerse ScienceDirect

Applied Catalysis B: Environmental

journal homepage: www.elsevier.com/locate/apcatb

Photocatalytic activity of a porphyrin/TiO_2 composite in the degradation of pharmaceuticals

Sharon Murphy[a], Carla Saurel[a], Anne Morrissey[b], John Tobin[c], Michael Oelgemöller[d], Kieran Nolan[a,*]

[a] School of Chemical Sciences, Dublin City University, Glasnevin, Dublin 9, Ireland
[b] Oscail, Dublin City University, Glasnevin, Dublin 9, Ireland
[c] School of Biotechnology, Dublin City University, Glasnevin, Dublin 9, Ireland
[d] School of Pharmacy and Molecular Sciences, James Cook University, Queensland, Australia

ARTICLE INFO

Article history:
Received 23 September 2011
Received in revised form 1 February 2012
Accepted 23 February 2012
Available online 3 March 2012

Keywords:
TiO_2
Tetra-(4-carboxyphenyl)porphyrin
Famotidine
Photocatalysis
Visible light

ABSTRACT

Two separate methods were used to prepare a tetra(4-carboxyphenyl)porphyrin (TCPP)-TiO_2 composite. In method A TCPP was absorbed onto TiO_2 in methanol at room temperature, whilst in method B TCPP was absorbed onto TiO_2 in dimethylformamide (DMF) at reflux. Both composites exhibited the same physical and chemical characteristics as shown by FT-IR, SEM and UV–vis diffuse reflectance spectroscopy (DRS). The photocatalytic activity of both composites was then determined by HPLC monitoring of the photo-degradation of the pharmaceutical Famotidine under both visible and solar light irradiation. The recyclability of the composites was also examined by recovery of the composite post-reaction, although the absorbed TCPP was found to partially degrade, the recycled composite still exhibited catalytic behaviour. All reactions were monitored by HPLC which revealed that the photodegradation of Famotidine by the TCPP–TiO_2 composites does not lead to complete mineralisation, but instead generates a range of intermediates/products. Investigation of these products by LC–MS–MS and DI–MS analysis found that one major degradation product was formed, the S-oxide of Famotidine. The TCPP–TiO_2 composites were also screened in the photo-degradation of the pharmaceuticals tamsulosin and solifenacin using the optimised conditions developed for famotidine. However, the composites were found to be ineffective for the photo-catalytic degradation of these compounds, demonstrating that this class of composite are only effective for specific compounds.

1. Introduction

In recent years, the presence of pharmaceuticals in the environment has become a serious cause for concern and the problem is continuing to grow with the on-going development of more potent and more metabolically resistant drugs [1]. There are a number of point-sources for the entry of drugs to the environment and these include: (i) direct entry of pharmaceuticals which are out-of-date or unused in refuse or down the toilet, (ii) excretion by patients whilst on drug therapy, (iii) wastewater from pharmaceutical production plants, municipal wastewater treatment plants and hospital effluents, and (iv) excreted veterinary drugs in manure which can then leach into soil [2]. These intact or partially degraded pharmaceuticals (and their metabolites) can further be present in agricultural run-off from soil, effluent from treatment plants and effluent from landfill sites where they can inevitably end up in ground and surface waters [3].

A significant body of research has been devoted to tackling this issue, employing the use of advanced oxidation processes (AOPs). Of these AOP processes, those which use the photocatalyst TiO_2 are some of the most studied for pharmaceutical abatement. TiO_2 is an effective photocatalyst and is cheap, safe and regularly used in the pharmaceutical, food and cosmetic industries [4,5]. It can also be employed in either a suspended or immobilised form with advantages and disadvantages to both configuration systems. Although this process is quite effective alone, it is usually used in conjunction with an auxiliary oxidant to ensure complete mineralisation [6,7]. Countless literature articles exist documenting its efficient degradation of a wide range of dyes, pesticides and pharmaceutical compounds [8,9]. In the past decade however, research in this area has been focused on the development of visible light sensitised (VLS) photocatalytic materials which incorporate TiO_2 and which serve to extend its absorption into the visible region. Alternative visible light sources such as halogen lamps and sustainable solar light can thus be harnessed. Recent examples of titania sensitised with visible light absorbing molecules include methylene blue, rhodamine B [10], and Chryosidine G [11]. In addition to these, macrocyclic sensitizing molecules such as phthalocyanines

* Corresponding author. Tel.: +353 1 700 5913.
E-mail address: Kieran.Nolan@dcu.ie (K. Nolan).

0926-3373/$ – see front matter © 2012 Elsevier B.V. All rights reserved.
doi:10.1016/j.apcatb.2012.02.027

Table 1
Structures and therapeutic class of selected pharmaceutical targets.

Name	Therapeutic class	Structure	Mol. wt. (g/mol)
Famotidine	H_2-receptor anatagonist	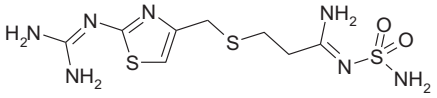	337.44
Solifenacin succinate	Anticholinergic muscarinic receptor antagonist	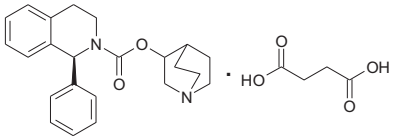	480.55
Tamsulosin HCl	α1-Adrenoreceptor antagonist	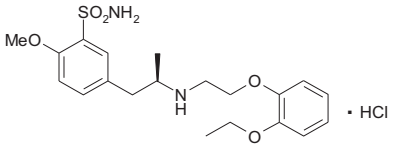	444.45

and porphyrins in their free [12] and metallated forms have also been applied [13,14]. The photocatalytic activity of these materials have thus far been examined exclusively on target molecules such as the textile dye methylene blue [11], and nitrophenols [15,16]. No studies yet exist, to our knowledge, on the efficacy of these materials on actual pharmaceuticals.

Recently, a TiO_2 based composite was prepared by Li et al. with the porphyrin tetra-(4-carboxyphenyl)porphyrin (TCPP) [12,22]. Their work reported the efficiency of this composite in the degradation of Acid Chrome Blue K. In this article, we have prepared the same composite using the method previously reported, and compared it with an alternative coating method based on simple adsorption of the dye to the titania. We have characterised both composites with FT-IR and UV–vis DRS and evaluated the photoactivity of this composite with the pharmaceutical famotidine, a histamine H_2-receptor antagonist used in the treatment of peptic ulcer disease. In patients that use famotidine, it has been documented that of the administered dose, between 65 and 70% of the parent compound is found unchanged in the urine [17]. This indicates that this drug is one of the many compounds released into the environment on a day-to-day basis. Further to this, we have conducted photocatalytic experiments both indoor with halogen tungsten lamps and outdoor using natural Irish solar conditions and we have also assessed the possibility of reuse of the material post-reaction. In addition to this, we have tested the performance of the composite with two other pharmaceuticals: tamsulosin (an antagonist of alpha 1-adrenoreceptors used in relieving the symptoms of benign prostatic hyperplasia) and solifenacin (an anticholinergic muscarinic receptor antagonist used in the treatment of overactive bladder). This, to our knowledge, is the first use of sensitised TiO_2 via functionalised porphyrin to be tested on pharmaceuticals.

2. Experimental

2.1. Materials

P-25 TiO_2 was kindly donated by Degussa, tetra-(4-carboxyphenyl) porphyrin was purchased from Porphyrin Systems (Germany) and was used as received. Famotidine, tamsulosin and solifenacin were donated from Astellas in Dublin, Ireland. Table 1 shows the structure, therapeutic class and molecular weight of the three pharmaceuticals. HPLC grade solvents were purchased from Fischer Scientific (Ireland). Nylon filter membranes purchased from Millipore (Dublin, Ireland) were used for filtration of photocatalytic samples prior to HPLC analysis.

2.2. Analysis and spectroscopic methods

IR spectra were recorded on a PerkinElmer Spectrum 100 FT-IR spectrometer using ATR (diamond) or an FT-IR PerkinElmer (GX–FTIR) with preparation using KBr discs. UV–vis spectra were attained using a Varian Cary 50 UV–vis spectrophotometer. Spectra were attained using a scan range of 200–900 nm. Scanning electron microscopy was performed with a Hitachi S3400 scanning electron microscope. UV–vis diffuse reflectance spectra (DRS) were attained using a Jasco V-670 UV/vis/NIR Spectrophotometer with a diffuse reflectance integrating sphere. Samples were prepared into discs with KBr, and the scan range was between 200 and 900 nm. The reflectance was converted to absorbance using the software, and plotted as the inv of % reflectance. HPLC analysis was performed on a Varian Prostar HPLC-PDA with a Varian Prostar Solvent Delivery system (model 230), PDA detector (model 330) and autosampler (model 410). Liquid chromatography–mass spectrometry (LC–MS) analysis was performed on an Agilent 1100 series high performance liquid chromatograph with a vacuum degasser, binary pump and autosampler. This was coupled to an AB Sciex API 2000 Triple Quadrupole Mass Spectrometer. DI–MS were also conducted with this mass spectrometer and 100 μL sample was injected with an automated syringe pump injector at a rate of 3 μL/min. Further instrument operating parameters can be found in Supplementary information.

2.3. Preparation of coated materials: TCPP–TiO_2-A and TCPP–TiO_2-B

2.3.1. TCPP–TiO_2-A

Methanol (50 mL) was added to a 100 mL round bottomed flask with a stirring bar. TiO_2 (1 g) was then added and the solution sonicated for 10 min. Tetra-(4-carboxyphenyl)porphyrin (0.05 g, 0.063 mmol) was then added. The solution was stirred at r.t. for 4 h. The product was then filtered and washed with methanol until the washings ran clear. After grinding with pestle and mortar the product was a purple/brown powder. The product was then analysed by FT-IR spectroscopy, diffuse reflectance UV–vis spectroscopy and SEM.

2.3.2. TCPP–TiO_2-B

This composite was prepared in a method previously described by Li et al. [12]. Dimethylformamide (DMF) (50 mL) was added to a 100 mL round bottomed flask with a stirring bar. TiO_2 (1 g) was then added along with tetra-(4-carboxyphenyl)porphyrin (0.05 g,

0.063 mmol). The solution was then heated to reflux for 5 h. The product was filtered and washed with DMF. The filtrate remained coloured after multiple washings. Soxhlet extraction was then performed overnight with methanol as the extraction solvent. The product was then left to dry on vacuum. After grinding with pestle and mortar the product was a purple/brown powder. The product was then analysed by FT-IR spectroscopy, diffuse reflectance UV–vis spectroscopy and SEM.

2.4. Photocatalytic reactions

Photocatalytic reactions were performed in Schlenk flasks with cold fingers and with 100 mL aqueous solutions of pharmaceutical (0.083 mM) and 0.031 g of photocatalyst. The photocatalytic reaction set-up can be found in Supplementary material. The reaction solution was sonicated for 10 min, and then irradiated with stirring at a distance of 28 cm from a 500 W halogen lamp (IQ Group). The illuminance of the halogen lamp was measured using a lux meter and was found to be 1649FC (17,760 lx). The emission spectrum of the halogen lamp is presented in Supplementary material. Solar photocatalytic reactions were performed in a similar manner with the reactor set-up taken outside post ultrasonication and with a lux meter recording light intensity. Experiments were conducted on the 22-06-2010 between 12 and 3 pm (intensity of the sunlight recorded on a lux meter throughout the experiment can be found in Supplementary data). All samples from photocatalytic reactions were filtered using Nylon filter membranes straight into vials for HPLC analysis. Composites were recovered from the reaction solution post irradiation via centrifuge and washed with water (3×10 mL) and methanol (3×10 mL). Remaining solvent was removed by rotary evaporator. Chromatographic separations were achieved on a Varian HPLC-PDA system with a Phenomenex RP PFP-column (4.6 mm × 150 mm). 20 μL Injection volumes were employed and a flow rate of 1 mL/min. For famotidine, a mobile phase of 9:91 methanol:water (0.1% formic acid) with detection at 265 nm was employed. Run time was 15 min with famotidine eluting at 10 min. For solifenacin, 30:70 acetonitrile:water (0.1% formic acid) with detection at 220 nm was employed. Run time was 22 min with solifenacin eluting at 14 min. For Tamsulosin, 40:60 methanol:water (0.1% formic acid) with detection at 223 nm was employed. Run time was 20 min with Tamsulosin eluting at 10 min. LC–MS analysis of famotidine was conducted on a Phenomenex RP PFP column (2.1 mm × 150 mm) with a mobile phase of 1:99 methanol:water (0.1% formic acid). 10 μL injection volumes were employed with a flow rate of 0.3 mL/min. Run time was 50 min with famotidine eluting at 29 min. Control experiments with TCPP (0.001 g) alone with no TiO_2 and both TCPP (0.001 g) and TiO_2 (0.031 g) were added together to see the combined effect compared to both TCPP–TiO_2 composites.

2.5. Calculation of photocatalytic efficiency

The degradation rate of pharmaceuticals in the reaction process was calculated using the following formula:

$$\text{Degradation rate} = \left(\frac{C_t}{C_0}\right)$$

where C_t is the concentration of pharmaceutical at time t, and C_0 is the initial concentration of pharmaceutical (0.083 mM) at the start of the reaction.

3. Results and discussion

3.1. Preparation of coated materials

Two different methods were adopted in the preparation of TCPP–TiO_2 composite materials. In the first method, TCPP was immobilised by simple adsorption and the alternative preparation was a reflux in DMF for 4 h as previously described by Li et al. [12] Both methods yielded an identical product which was a dark purple/brown powder (see Supplementary material). As a control experiment, non-functionalised TPP was left to stir in chloroform for 4 h to see if immobilisation was possible without carboxyl groups anchoring the sensitiser to TiO_2. This experiment yielded a white product indicating that no TPP had attached to the TiO_2 and demonstrated the necessity for carboxyl groups to anchor the dye to the TiO_2. Binding of the sensitiser to TiO_2 would be predicted to be monodentate as in dye sensitised solar cell models [18]. However, other modes of binding are possible such as hydrogen bonding, electrostatic, bidentate bridging and bidentate chelating, examples of which have been presented elsewhere [19].

Both procedures were repeated with a soxhlet extraction performed on both to determine the residual porphyrin content and thus determine the loading of porphyrin onto 1 g of TiO_2. For TCPP–TiO_2-A, approximately 0.035 g was recovered via soxhlet from the original 0.050 g used in the reaction. This would indicate a loading of 0.015 g/1 g TiO_2. For TCPP–TiO_2-B, 0.025 g was recovered leaving a loading of 0.025 g/1 g TiO_2 which is close to that obtained by Li et al. who reported a loading of 0.021 g/1 g TiO_2 through recovery of the residual TCPP from their product. It was noticed that when placed in water the colour of the composite went from purple/brown to green. Odobel et al. noticed a colour change of the porphyrin to green upon adsorption of the porphyrin to TiO_2 electrodes and attributed this effect to the interaction of the pyrrole nitrogens with the hydroxylic groups on the surface of the TiO_2 [20]. We believe that upon addition to the aqueous famotidine solution the same effect is occurring. Additionally the same effect occurred in the presence of acid. Upon removal of water and addition of methanol to the composite, it reverted back to its purple colour.

3.2. FT-IR analysis

FT-IR analysis was performed on both TCPP–TiO_2-A, TCPP–TiO_2-B and also on TCPP alone. Principle stretches for all samples are shown in Table 3 [21]. The ν(C═O) band at 1685 cm^{-1} in TCPP, is shifted to lower wavenumbers at 1614 cm^{-1} and 1621 cm^{-1} for TCPP–TiO_2-A and TCPP–TiO_2-B respectively. This 7 cm^{-1} difference between the ν(C═O) band in A and B could indicate different binding modes of the carboxylate to the TiO_2 surface based on the different methods of preparation or it could indicate different orientations of the porphyrin on the TiO_2 surface (i.e. binding through one carboxylate group, or two). The corresponding ν(C—O) band which can normally appear at 1210–1320 cm^{-1}, appears at 1222 cm^{-1} in TCPP and is again shifted with the coated TiO_2 samples to 1263 cm^{-1} for both. These shifts in the ν(C═O) and ν(C—O) bands were accompanied by a decrease in the intensity of these bands, which is indicative of an adsorption to TiO_2 according to work by Diaz-Uribe et al. [22]. TiO_2 bands are also clearly present in the spectra at 3400 cm^{-1} for ν(Ti—OH) and more significantly the very broad Ti—O—Ti stretch at ~600 cm^{-1} [23].

3.3. UV–vis spectroscopy

Fig. 1 shows the UV–vis spectra of the prepared photocatalytic materials compared with the uncoated P-25 TiO_2 and the free porphyrin. TiO_2 absorbs in the UV region below 400 nm.

Table 2
Shifts in the UV–vis samples for TCPP–TiO_2-A, TCPP–TiO_2-B, TCPP.

Characterisation of materials by UV–vis spectroscopy						
Sample	UV	Soret band (nm)	Q bands (nm)			
TCPP–TiO_2-A	Solid	408	523	560	597	654
TCPP–TiO_2-B	Solid	410	523	561	598	655
TCPP	Solid	411	523	560	596	654
TCPP	Methanol	416	512	547	589	643
TCPP	Ethanol (lit.)	419	514	548	588	645
TCPP	DMF (lit.)	418	515	549	591	646

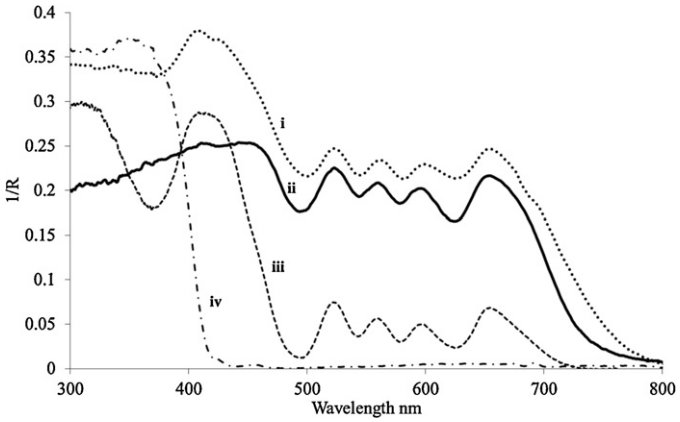

Fig. 1. UV–vis spectroscopy data for TCPP–TiO_2-B (i) TCPP (ii) TCPP–TiO_2-A (iii) and TiO_2 (iv).

TCPP–TiO_2–A, TCPP–TiO_2–B samples show almost identical spectra to each other and show Q bands at 523 nm, 560 nm, 597 nm 654 nm for TCPP–TiO_2-A and 523 nm, 561 nm, 598 nm and 655 nm for TCPP–TiO_2-B. The presence of these Q and soret bands in DRS spectra for the composites are indicative of the extension of the absorbance spectra of TiO_2 into the visible region. The similarities between the spectra of both composites are a very promising sign that the much simpler preparation method of TCPP–TiO_2-A is as effective as the TCPP–TiO_2-B method. The DRS of the free porphyrin in the solid state shows multiple bands both in the UV and visible region, the Q bands can be seen much more clearly than the Soret and appear at 523 nm, 560 nm, 596 nm and 654 nm.

Table 2 contains the wavelengths of the Soret and Q bands for TCPP in methanol, and also the UV–vis in other solvents found in the literature, and those for the coated TiO_2 and free porphyrin samples in our DRS studies. The intensity of the Q-bands relative to one another in the DRS studies compared with those in the solution phase was explained in the differences between the two sampling techniques and the lack of solvent in solid state which can clearly influence the intensity and shifts of both the Soret and Q bands. Work by Diaz-Uribe et al. and Cherian and Wamser described a red shift for the coated TiO_2 samples when compared with the UV–vis in ethanol of TCPP [22,24]. Diaz reported a shift of approximately 8 nm in the Q bands, whereas Cherian reported a shift of 5 nm for the lower energy bands and 10 nm for the higher energy bands albeit that they coated TiO_2 electrodes. Ma et al. reported an average shift of 8 nm with their coated sample compared with the UV–vis of TCPP in DMF [25]. Ma et al. also reported a decrease in intensity of the Soret band relative to the Q-bands which is similar to what we have observed in this work.

3.4. SEM imaging

SEM images were attained for both samples and also for P-25 TiO_2 Fig. 2. The nanoparticulate nature of the P-25 standard can be seen compared with the prepared coated TiO_2 samples. The prepared coated samples also show identical textures relative to the P-25 sample.

3.5. Photocatalytic efficiency of TCPP–TiO_2 in famotidine degradation

Fig. 3A and B shows photocatalytic experiments in triplicate with each composite in the degradation of famotidine using a halogen lamp compared with controls of TiO_2 alone and photolysis (absence of any photocatalyst). It should be noted that a source of air or oxygen was not supplied in these photoreactions. These experiments were monitored using HPLC analysis. Both composites show similar degradation, with almost 100% elimination of famotidine after 3 h. However, it should be noted that there is a significant intermediate formed as determined by HPLC analysis. Both composite materials are significantly better than P-25 TiO_2, which only achieves ~10% elimination of famotidine after 3 h. This elimination by TiO_2 is more than would be expected because TiO_2 requires light below 400 nm to generate hydroxyl radicals however

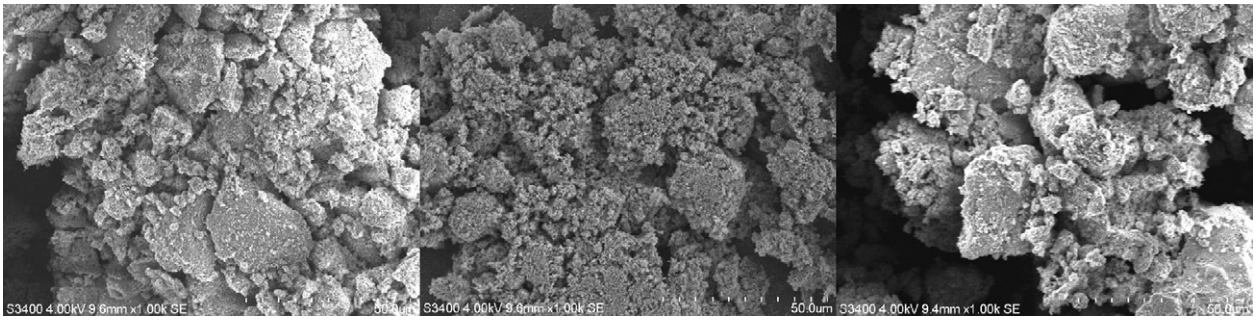

Fig. 2. SEM image of TCPP–TiO_2-B (left), P-25 TiO_2 and TCPP–TiO_2-A (right).

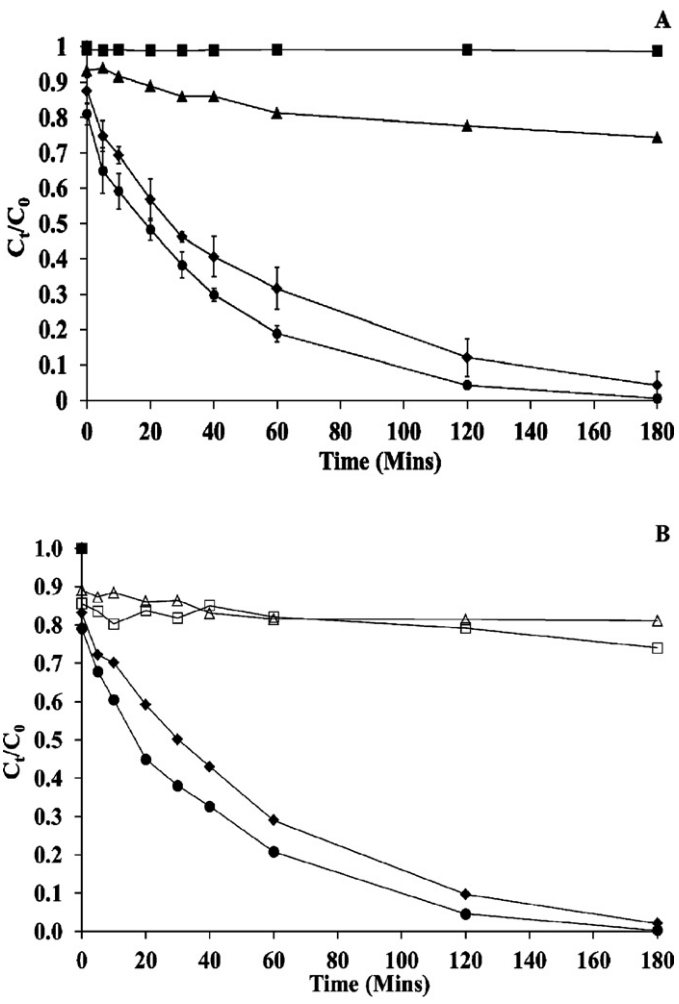

Fig. 3. Indoor photocatalytic experiments and controls with TCPP–TiO_2-A (●) and TCPP–TiO_2-B (♦), photolysis (■) P-25 TiO_2 (▲) TCPP (1 mg/100 mL) + P-25 TiO_2 (△) and TCPP (1 mg/100 mL). (□) With a halogen lamp for 3 h. [TCPP–TiO_2] or [P-25] = 0.031 g, [FAM] = 0.083 mM.

a tail of absorbance above 400 nm could give rise to some radical formation and lead to this degradation observed.[1] One other possibility for this activity could include the surface chemical interaction of famotidine with TiO_2 which may induce visible light absorption as reported with other pollutants [26], however we believe that the former possibility is most likely.

Fig. 3A also shows that the TCPP–TiO_2-A is superior in all 3 experiments, over the TCPP–TiO_2-B. We initially considered that this may be due to the presence of residual TCPP (un-anchored TCPP) as no soxhlet extraction was undertaken of the TCPP–TiO_2-A prior to use.[2] Fig. 3B shows a series of additional control experiments which were conducted. Two control experiments are shown with the sensitiser alone and also the sensitiser in the presence of TiO_2 compared with the performance of both composite materials. The amount of sensitiser used in these control experiments (0.001 g/1 g TiO_2) was more than double the amount coated onto 0.031 g of the composite. Considering a coating of 0.015 g/1 g TiO_2 as in TCPP–TiO_2-A, in 0.031 g of TCPP–TiO_2, there would be less than 0.0005 g of sensitiser. The sensitiser alone shows minimal degradation although degradation may have been expected due to singlet oxygen generation. A mechanism of photo-oxidative degradation in this manner is not expected with the TCPP–TiO_2 due to limited singlet oxygen generation [22,27]. TiO_2 alone also shows very poor degradation whilst in the presence of the sensitiser showing that binding of the sensitiser to the TiO_2 is required for photodegradation and that photodegradation is due to the composite material and not its individual components. Adsorption of famotidine onto the photocatalyst in the dark (for 1 h) was also minimal with no change in the concentration after the initial adsorption/dispersion of the photocatalyst (data not presented).

3.6. Recovering of the TCPP–TiO_2 materials and stability

After all photocatalytic experiments the composites were recovered from solution. In all cases, the recovered composites were beige in colour, differing from the initial purple/brown composite showing the apparent instability of the composite. Further experiments concluded the photodegradation of the porphyrin on the TiO_2 surface. There was no indication that the dye was being cleaved upon degradation. FT-IR analysis was performed on the composites post reaction and there are some noticeable differences between the samples. The ν(C=O) stretch which appeared at 1614 cm^{-1} and 1621 cm^{-1} for TCPP–TiO_2-A and TCPP–TiO_2-B respectively shifted to 1630 cm^{-1} and 1637 cm^{-1} (Supplementary data). Interestingly, the 7 cm^{-1} difference between the ν(C=O) stretch in A and B was maintained in these post reaction samples. The three stretches typical of TCPP in the fingerprint region shown in Fig. 4A and B are also noticeably different in Fig. 4C and D. The three bands are now overlapped by one principle band at 1062 cm^{-1} which would indicate significant changes to the core π-ring system. Any changes in this core ring system could indirectly contribute to the shift observed in the ν(C=O) band. DRS studies (Fig. 5) of the composite post reaction would indicate that the sensitiser remains somewhat intact on the surface of the TiO_2 despite the changes in the FTIR spectra. These samples were further used in photocatalytic experiments to examine whether photoactivity was retained.

3.7. Recycling of the porphyrin/TiO_2 composite

After recovering the composite post reaction we investigated whether it still had retained its photoactivity despite the degradation. It was washed, dried, and reintroduced into fresh famotidine solution and irradiated for another 3 h. The results are shown in Fig. 6. The photoactivity of the composite is now significantly reduced, although it is still superior over the standard P-25 TiO_2 photocatalyst and photolysis removing almost 67% of the original famotidine concentration. Additionally, it was observed that TCPP–TiO_2-A displayed a better activity over TCPP–TiO_2-B even in recycling. This behaviour was also observed in previous experiments.

3.8. Difference in photo-activity of TCPP–TiO_2-A and TCPP–TiO_2-B

The difference in photo-activity of both composites was seen only in the indoor halogen lamp experiments which would indicate a slight difference in the visible light absorption characteristics of the composites. Although both composites exhibited different loading capacities, their UV–vis solid state spectra showed no real discernible differences. On the other hand, in their IR spectra a difference of 7 cm^{-1} was constant between A and B for the ν(C=O)

[1] The P-25 TiO_2 used in these studies is a commercial standard consisting of approximately 80:20 anatase:rutile. The function of the rutile is to extend absorption over 400 nm, this may be giving rise to the degradation of Famotidine seen by visible light (to approximately 425 nm, see DRS for TiO_2 Fig. 1).

[2] Further work in which a soxhlet extraction of the composite (post-synthesis) was performed, indicated that it had the same performance as non-soxhlet extracted TCPP-TiO_2-A (Supplementary data).

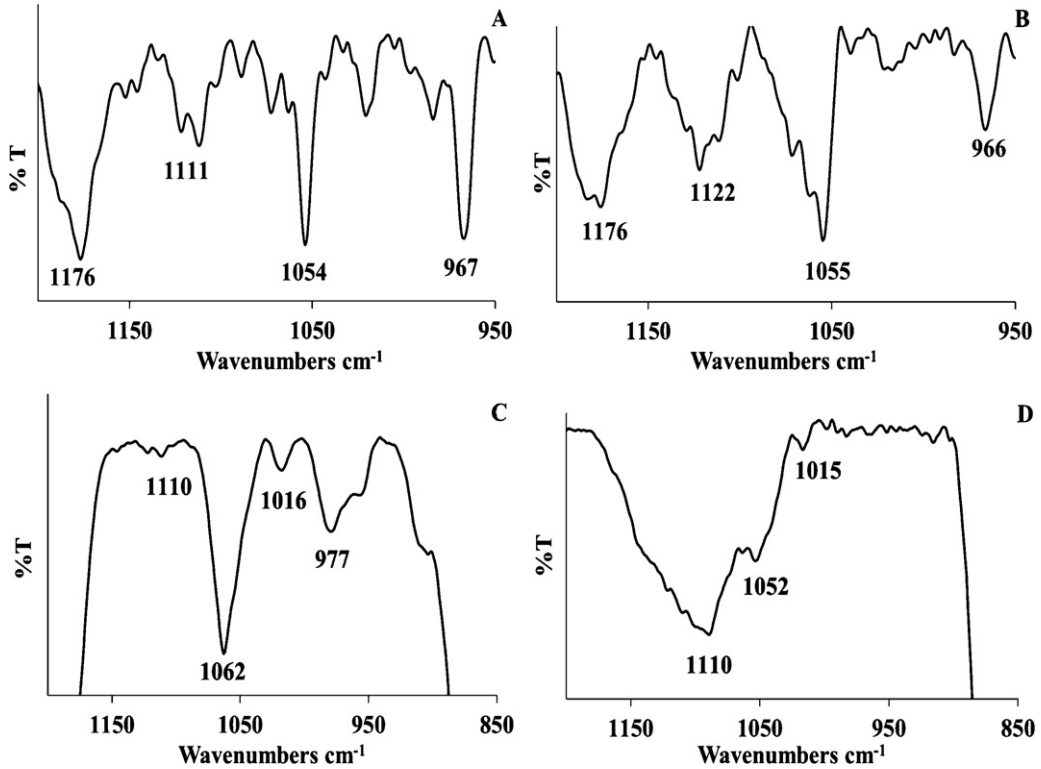

Fig. 4. FT-IR showing the fingerprint region for TCPP–TiO_2 composites pre/post-photoreaction. (A): TCPP–TiO_2-A (pre) (B): TCPP–TiO_2-B, (pre) (C): TCPP–TiO_2-A (post) (D): TCPP–TiO_2-B (post).

stretch in both the pre-reaction and post-reaction samples (see Table 3 and Section 3.6). This difference in shift and the differing loading capacities obtained for both composites could explain the difference in photo-activity. Depending on the binding mode or the orientation of the porphyrin on the TiO_2 surface, different loadings could therefore arguably be possible. Wang et al. reported recently that optimum loadings of sensitiser must be realised and overloading in particular can be detrimental to the photoactivity of the photocatalyst [28]. Also, different orientations of the porphyrin on the TiO_2 surface could lead to a stronger electronic communication between the porphyrin and the TiO_2 surface and could thus facilitate better electron injection to the TiO_2 conduction band.

3.9. Solar photocatalytic degradation efficiency of famotidine

A set of solar experiments were conducted using TCPP–TiO_2 A and B composites, P-25 TiO_2 and one control experiment (photolysis). The results shown in Fig. 7 are what we expected under solar conditions (The intensity of light, recorded on a lux meter during the experiment, varied between 2.8 and 11 FC (footcandles) with the fluctuations mainly due to cloud coverage.). Both TCPP–TiO_2 composites achieve 90% degradation of famotidine after 0.5 h. P-25 TiO_2 also achieved a significant degradation under solar conditions, (although slower than both composites initially) with the additional UV light present in solar light being attributed to this. Photolysis showed insignificant degradation. Both TCPP–TiO_2 A and B show identical activity is a promising result as they were both synthesised in different manners. However, 100% photodegradation of famotidine was not achieved in the experiments using TCPP–TiO_2 A and B, based on HPLC analysis. What is perhaps most interesting is that the HPLC traces for the two composites under solar light irradiation are identical to the HPLC traces of the halogen lamp experiments, indicating that the same intermediate is being formed under both experimental conditions (Supplementary data). Contrary to this the P-25 solar experiment gives complete elimination of famotidine with minimal intermediate production. It is

Table 3
FT-IR samples for TCPP, TCPP–TiO_2-A and TCPP–TiO_2-B, o = overlap, stretches referenced from work by Thomas et al. and Jiang et al.

Characterisation of materials by FT-IR spectroscopy						
Functional group	TCPP		TCPP–TiO_2-A		TCPP–TiO_2-B	
TCPP, C=C—H stretch phenyl	3014	Weak	3740	Weak	3743	Weak
TiO_2, surface —OH groups			3391	Strong	3410	Strong
	2524	Weak	2923	Medium	2925	Medium
TCPP, C=O anchor	1685	Strong	1614	Medium	1621	Medium
TCPP, C=C	1604	Strong	o		o	
TCPP, C—H band	1400	Medium	1383	Medium	1383	Weak
TCPP, C—O stretch	1222	Strong	1263	Weak	1263	Weak
TCPP, C_6H_5 substituted	1174	Strong	1176	Weak	1176	Weak
TCPP, p-subsitituted C_6H_5	1099	Strong	1110	Weak	1111	Weak
C—H pyrrole porphyrin ring system	o		1054	Weak	1055	Weak
TCPP, pyrole C—H (rocking)	963	Strong	967	Weak	966	Weak
TiO_2, Ti—O—Ti vibration			636	Strong	667	Strong

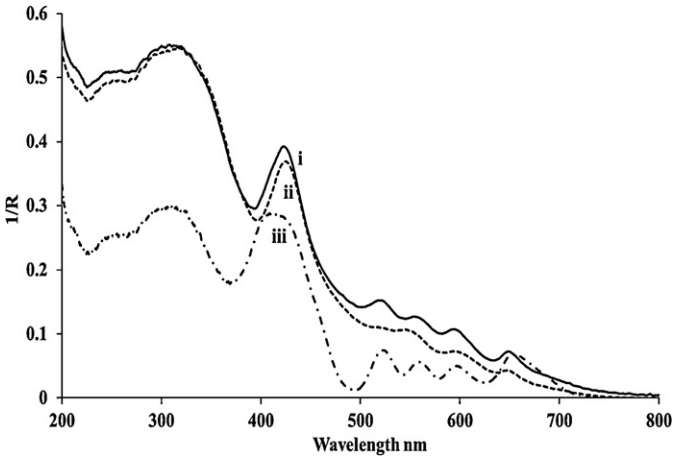

Fig. 5. UV analysis of TCPP–TiO_2-A (i) and TCPP–TiO_2-B (ii) post reaction compared with TCPP–TiO_2-A (iii) pre-reaction.

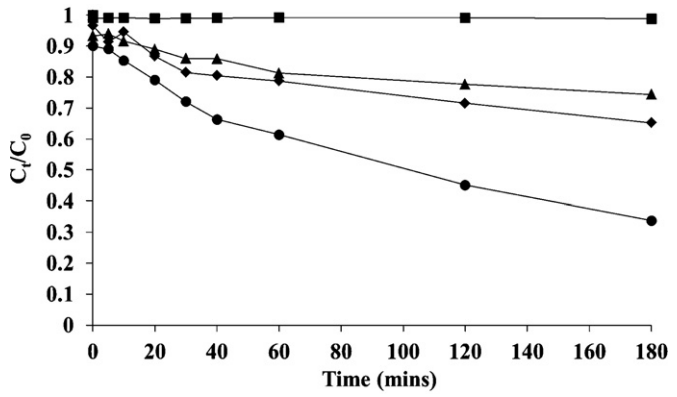

Fig. 6. Photocatalytic experiments with recycled composites compared with controls. TCPP–TiO_2-A (●) and -B (♦), photolysis (■) P-25 TiO_2 (▲). [TCPP–TiO_2] or [P-25 TiO_2] = 0.031 g, [FAM] = 0.083 mM.

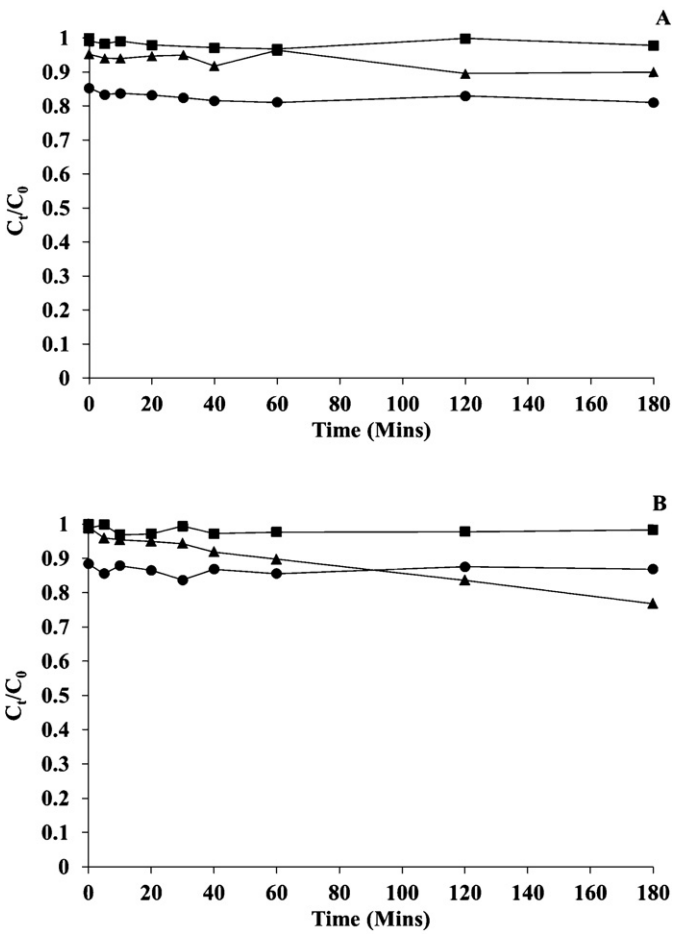

Fig. 8. Photocatalytic experiments with TCPP–TiO_2-A compared with controls for solifenacin (A) and tamsulosin (B). TCPP–TiO_2-A (●), photolysis (■), and P-25 TiO_2 (▲). [TCPP–TiO_2] or [P-25 TiO_2] = 0.031 g, [TAM], [SOL] = 0.083 mM.

evident that the mechanism of degradation of famotidine with the TCPP–TiO_2 composites A and B is different than with P-25.

3.10. Evaluation of the composite materials with tamsulosin and solifenacin

Further experiments were conducted with tamsulosin and solifenacin to examine the applicability of the photocatalyst to other pharmaceuticals. The results for de-capitalise Solifenacin are shown in Fig. 8A and for tamsulosin are shown in Fig. 8B. In the case of both pharmaceuticals, the performance of the TCPP–TiO_2 was not superior over TiO_2. After sonication and prior to irradiation there is a drop in the concentration of pharmaceutical which we believe is due to the dispersion of the photocatalyst and

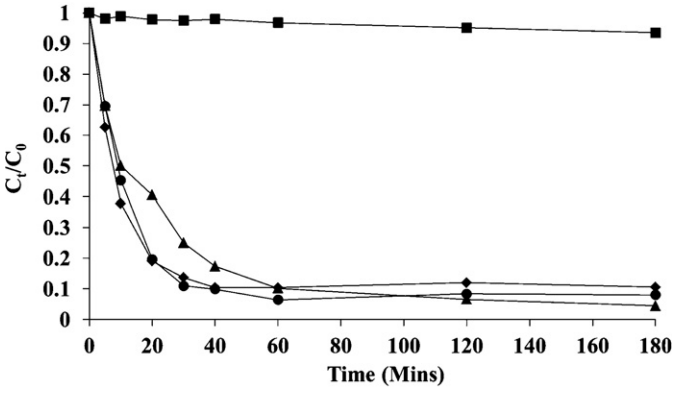

Fig. 7. Solar photocatalytic reactions performed on 22-06-2010. TCPP–TiO_2-A (●) and -B (♦), photolysis (■) P-25 TiO_2 (▲). [TCPP–TiO_2] or [P-25 TiO_2] = 0.031 g, [FAM] = 0.083 mM.

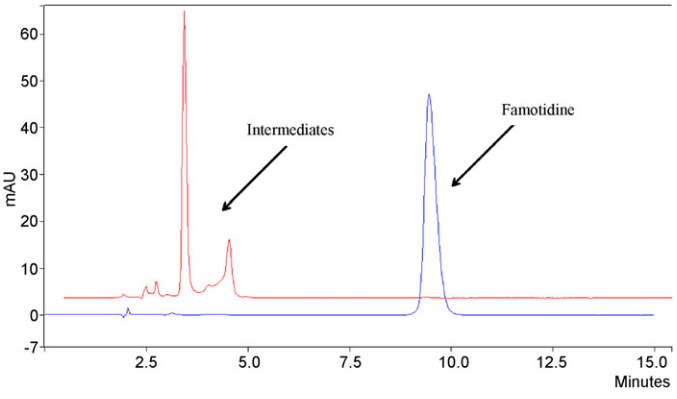

Fig. 9. HPLC chromatogram showing famotidine, at 0 min (blue) and after 180 min (red), in the photocatalytic degradation (indoor) by TCPP–TiO_2-A. [FAM] = 0.083 mM, TCPP = 0.031 g. (For interpretation of the references to colour in this figure legend, the reader is referred to the web version of the article.)

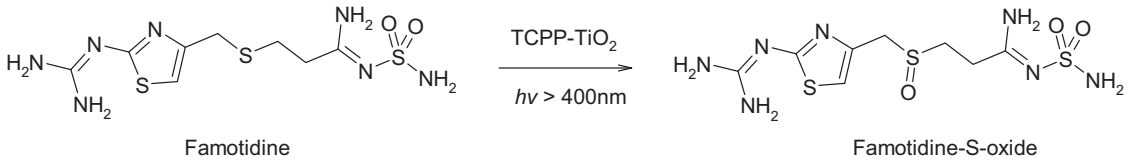

Fig. 10. Famotidine oxidation product, famotidine-S-oxide, which is also an in vivo metabolite.

adsorption of the pharmaceutical to the photocatalyst. However, at the point of exposure of the reaction solution to light irradiation there is no significant drop in concentration which indicates no photo-degradation is occurring. In addition, P-25 TiO_2 and photolysis in the case of both pharmaceuticals did not yield any significant degradation after the 3 h period.

Solifenacin and tamsulosin both contain a number of aromatic rings which can be difficult to degrade, which may explain why the photocatalyst is superior in the case of famotidine and not in the case of tamsulosin and solifenacin. Applicability of this photocatalyst can thus be considered to be unsuitable perhaps for drugs with significant aromatic/phenyl groups, although this would further have to be evaluated in follow-up studies.

3.11. Identification of famotidine's degradation product

HPLC chromatograms of famotidine experiments (Fig. 9) showed significant quantities of intermediates which may imply a selective oxidation(s) is simply occurring and not a degradation of the compound. Famotidine undergoes partial oxidation in the body forming exclusively the S-oxide metabolite (Fig. 10). LC–MS analysis was conducted on samples from the photocatalytic experiments and MS/MS analysis was performed on the main degradation product found in these analyses. Extracted ion chromatograms (XICs) from the 0 min and 180 min samples are shown in Fig. 11 and in Supplementary information. This data indicated that there was no presence of famotidine after 180 min and showed a significant presence of one degradation product at a mass of $m/z = 354$. This main degradation product was identified as the S-oxide of famotidine and the mass spectrum in Fig. 12 shows the parent mass, $m/z = 354$ and fragment ions $m/z = 275$, 205 and 155. Structures for these ions are given in Fig. 13. We postulated that oxidation to this product was likely in our studies due to the similarities between photocatalytic oxidation of organic compounds and phase 1 metabolism in vivo. Photocatalytic oxidation of related H_2 receptor antagonists, such as ranitidine and cimetidine, have also shown oxidation at this site [29,30]. Identification of this product confirms unequivocally that this composite can only selectively oxidise famotidine at the thioether site. Since the other pharmaceuticals, tamsulosin and solifenacin do not contain a thioether moiety, no degradation or conversion is seen.

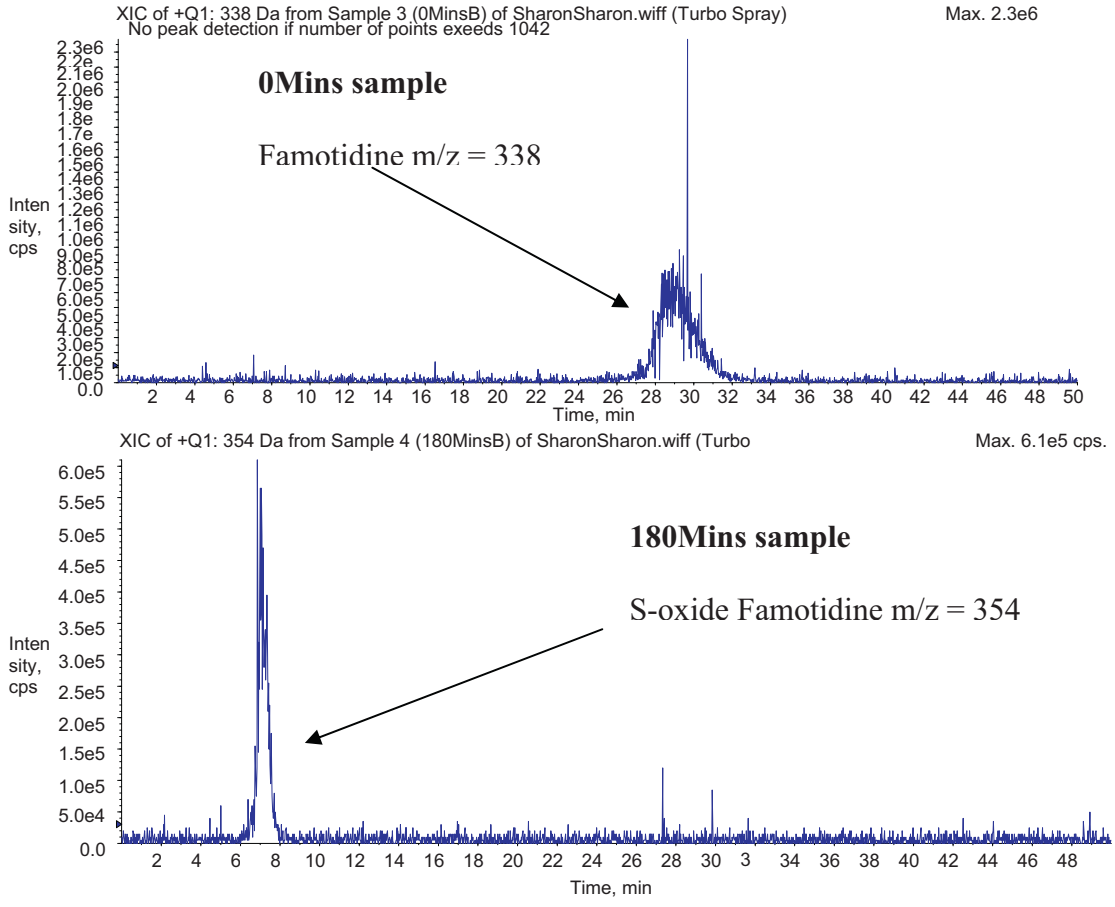

Fig. 11. XICs of the photocatalytic degradation reaction of famotidine (indoor) with TCPP–TiO_2 at 0 min and 180 min.

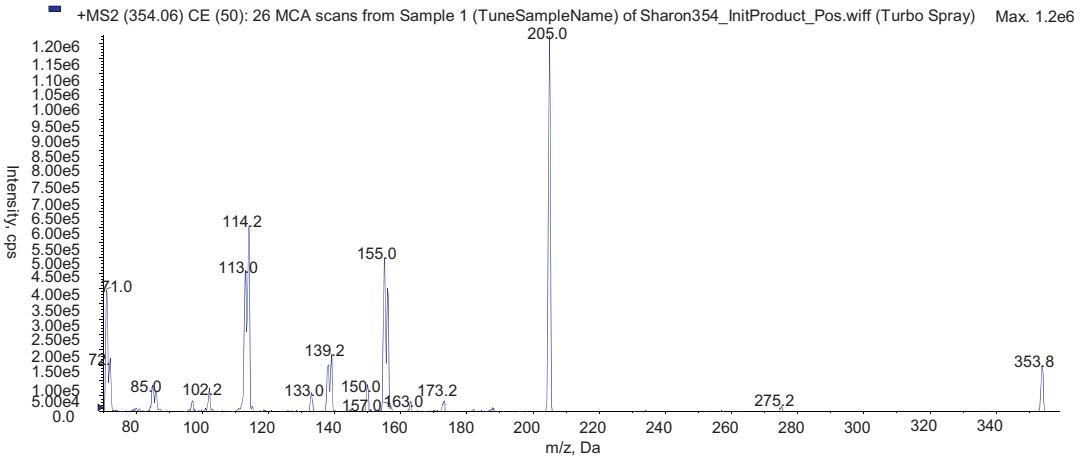

Fig. 12. Mass spectrum of $m/z = 354$ showing the parent mass and fragments for the principle intermediate formed from photocatalysis with TCPP–TiO_2.

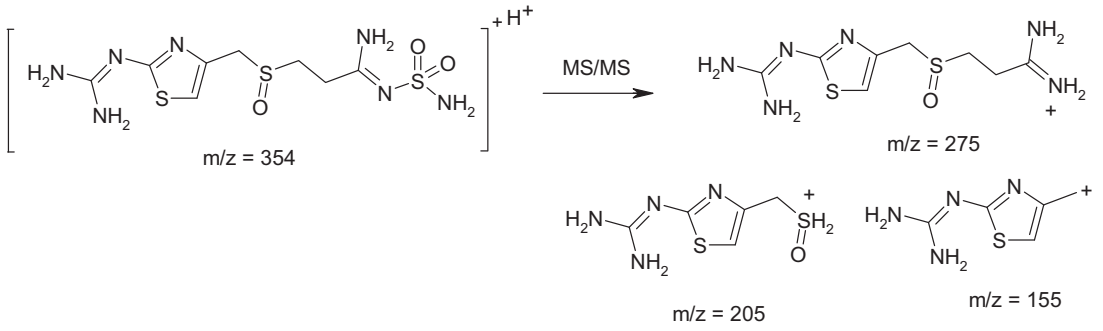

Fig. 13. Structure of the degradation product $m/z = 354$ and its fragment ions $m/z = 275$, 205 and 155.

3.12. Mechanism of famotidine degradation with TCPP–TiO_2 composites A and B

The exact mechanism of photodegradation via visible light sensitised TiO_2 composites is still unclear. A number of mechanisms have been proposed by various authors, which include electron transfer/injection with subsequent formation of reactive oxygen species (ROS), or directly via a sensitiser-only generated singlet oxygen mechanism [16,31,32]. These mechanisms are both presented in the following equations for TCPP–TiO_2:

Electron injection and formation of ROS:

$$[\mathrm{TCCP} - \mathrm{TiO_2}] \xrightarrow{h\nu} [\mathrm{TCPP^+} - \mathrm{TiO_2}(e_{CB})]*$$

$$[\mathrm{TCCP^+}\text{–}\mathrm{TiO_2}(e_{CB})]* + \mathrm{O_2} \rightarrow [\mathrm{TCCP^+}\text{–}\mathrm{TiO_2}] + \mathrm{O_2^{\bullet -}}$$

$$\mathrm{O_2^{\bullet -}} + \mathrm{Famotidine} \rightarrow \mathrm{S\text{-}Oxide\ of\ Famotidine}$$

Singlet oxygen mechanism:

$$[\mathrm{TCCP} - \mathrm{TiO_2}] \xrightarrow{h\nu} [\mathrm{TCPP^1} - \mathrm{TiO_2}]$$

$$[\mathrm{TCCP^1} - \mathrm{TiO_2}] \xrightarrow{\mathrm{ISC}} [\mathrm{TCPP^3} - \mathrm{TiO_2}]$$

$$[\mathrm{TCPP^3} - \mathrm{TiO_2}] + \mathrm{O_2^3} \rightarrow [\mathrm{TCPP} - \mathrm{TiO_2}] + \mathrm{O_2^1}$$

$$\mathrm{O_2^1} + \mathrm{Famotidine} \rightarrow \mathrm{S\text{-}Oxide\ of\ Famotidine}$$

Both mechanisms are possible, and both would explain the observed sulfoxidation product, however, electron injection from the sensitiser directly into the conduction band of TiO_2 is generally the most accepted mechanism [4,22,27,33–35]. Furthermore, the reactive species generated via this mechanism is the superoxide radical anion which has been shown to selectively oxidise benzyl sulfides to sulfoxides [34,35]. We also believe that singlet oxygen may not be involved based on our control studies with the attempted photooxidation of famotidine with TCPP on its own (Fig. 3B), as no oxidation of famotidine was observed in this reaction.

4. Conclusions and future work

A visible light sensitised photoactive composite incorporating P-25 TiO_2 and the sensitiser tetra-(4-carboxyphenyl) porphyrin has been prepared via adsorption at room temperature and compared to a literature method. UV–vis analysis of the prepared composites indicated that the porphyrin dye in both composites extended the absorption of TiO_2 into the visible region such that solar and visible light could be harnessed. FTIR analysis indicated successful binding of the dye to the TiO_2 surface. Examination of the photocatalytic activity of the composite materials on the pharmaceutical famotidine with a halogen lamp showed superior degradation over the standard P-25 TiO_2. In addition, solar experiments were conducted and demonstrated an enhanced efficacy of the composite

over TiO_2 under the same conditions. It was also demonstrated that the composite, although partially photo-bleached, can be recovered and recycled. HPLC chromatograms from the photocatalytic experiments show that the degradation of famotidine using the TCPP–TiO_2 composites did not give complete mineralisation and further LC–MS analysis indicated that a selective oxidation of the famotidine molecule was occurring. This oxidation product was confirmed with MS/MS analysis to be the S-oxide of famotidine. The performance of the composite was further evaluated with the pharmaceuticals solifenacin and tamsulosin, however, the composite was ineffective in degrading these pharmaceuticals demonstrating that these composites are substrate specific.

Acknowledgements

The authors would like to acknowledge the NCSR and DCU for use of equipment, and SFI (grant 07/RFP/EEEOBF768) for their financial support in this project. Sincere thanks are also due to Dr. James J. Walsh and Prof. Tia E. Keyes for assistance with DR UV measurements.

Appendix A. Supplementary data

Supplementary data associated with this article can be found, in the online version, at doi:10.1016/j.apcatb.2012.02.027.

References

[1] S.K. Khetan, T.J. Collins, Chem. Rev. 107 (2007) 2319–2364.
[2] K. Kümmerer, Pharmaceuticals in the Environment: Sources, Fate, Effects and Risks, second ed., Springer Publications, 2005.
[3] E. Zuccato, S. Castiglioni, R. Fanelli, J. Hazard. Mater. 122 (3) (2005) 205–209.
[4] A.L. Linsebigler, G. Lu, J.T. Yates, Chem. Rev. 95 (1995) 735–758.
[5] C. Chawengkijwanich, Y. Hayata, Int. J. Food Microbiol. 123 (2008) 288–292.
[6] O. Legrini, E. Oliveros, A.M. Braun, Chem. Rev. 93 (1993) 671–698.
[7] E.S. Elmolla, M. Chaudhuri, Desalination 252 (2010) 46–52.
[8] B.N. Lee, W.D. Liaw, J.C. Lou, Environ. Eng. Sci. 163 (1999) 165–175.
[9] H.M. Coleman, B.R. Eggins, J.A. Byrne, F.L. Palmer, E. King, Appl. Catal. B Environ. 24 (2000) L1–L5.
[10] D. Chatterjee, A. Mahata, J. Photochem. Photobiol. A 153 (2002) 199–204.
[11] D. Jiang, Y. Xu, D. Wu, Y. Sun, J. Solid State Chem. 181 (2008) 593–602.
[12] D. Li, W. Dong, S. Sun, A. Shi, S. Feng, J. Phys. Chem. C 112 (2008) 14878–14882.
[13] Q. Sun, Y. Xu, J. Phys. Chem. C 113 (2009) 12387–12394.
[14] X. Lü, J. Li, C. Wang, M. Duan, Y. Luo, G. Yao, J. Wang, Appl. Surf. Sci. 257 (2010) 795–801.
[15] G. Mele, R. Del Sole, G. Vasapollo, E. Garcia-Lopez, L. Palmisano, M. Schiavello, J. Catal. 217 (2003) 334–342.
[16] M. Duan, J. Li, G. Mele, C. Wang, X. Lu, G. Vasapollo, F. Zhang, J. Phys. Chem. C 114 (2010) 7857–7862.
[17] K.W. Lee, S.R. Kayser, R.H. Hongo, Z.H. Tseng, M.M. Scheinman, Am. J. Cardiol. 93 (2004) 1325–1327.
[18] M. Gratzel, Inorg. Chem. 44 (2005) 6841–6851.
[19] Q. Qu, H. Geng, R. Peng, Q. Cui, X. Gu, F. Li, M. Wang, Langmuir 26 (12) (2010) 9539–9546.
[20] F. Odobel, E. Blart, M. Lagree, M. Villieras, H. Boujtita, N. El Murr, S. Caramori, C.A. Bignozzi, J. Mater. Chem. 13 (2003) 502–510.
[21] D.W. Thomas, A.E. Martell, J. Am. Chem. Soc. 78 (1956) 1338–1343.
[22] C.E. Diaz-Uribe, M.C. Daza, F. Martínez, E.A. Paez-Mozo, C.L.B. Guedes, E. Di Mauro, J. Photochem. Photobiol. A 215 (2010) 172–178.
[23] D. Jiang, Y. Xu, B. Hou, D. Wu, Y. Sun, J. Solid State Chem. 180 (5) (2007) 1787–1791.
[24] S. Cherian, C. Wamser, J. Phys. Chem. B 104 (2000) 3624–3629.
[25] T. Ma, K. Inoue, H. Noma, K. Yao, E. Abe, J. Photochem. Photobiol. A 152 (2002) 207–212.
[26] S. Kim, W. Choi, J. Phys. Chem. B 109 (2005) 5143–5149.
[27] W. Li, N. Gandra, E.D. Ellis, S. Courtney, S. Li, E. Butler, R. Gao, Appl. Mater. Interfaces 1 (2009) 1178–1784.
[28] C. Wang, J. Li, G. Mele, M. Duan, X. Lu, L. Palmisano, G. Vasapollo, F. Zhang, Dyes Pigments 84 (2010) 183–189.
[29] J. Radjenović, C. Sirtori, M. Petrović, D. Barceló, S. Malato, Chemosphere 79 (2010) 368–376.
[30] J.M. Buth, W. Arnold, K. McNeill, Environ. Sci. Technol. 41 (2007) 6228–6233.
[31] C. Wang, G. Yang, J. Li, G. Mele, R. Slota, M.A. Broda, M. Duan, G. Vasapollo, X. Zhang, F. Zhang, Dyes Pigments 80 (2009) 321–328.
[32] H. Huang, X. Gu, J. Zhou, K. Ji, H. Liu, Y. Feng, Catal. Commun. 11 (2009) 58–61.
[33] J. Zhang, L. Zhang, X. Li, S. Kang, J. Mu, J. Dispersion Sci. Technol. 32 (2011) 943–947.
[34] S.M. Bonesi, M. Fagnoni, A. Albini, Eur. J. Org. Chem. (2008) 612–2620.
[35] E.L. Clennan, Acc. Chem. Res. 34 (2001) 875–884.